

## Soft Gamma Rays Emitted by Nuclei in the Capture of Thermal Neutrons

I. V. ESTULIN, L. F. KALINKIN, A. S. MELIORANSKII

*Moscow State University*

(Submitted to JETP editor December 26, 1956)

J. Exptl. Theoret. Phys. (U.S.S.R.) 32, 979-992 (May, 1957)

A luminescent spectrometer was used to measure the energy and absolute intensities of gamma rays emitted by  $\text{Co}^{59}$ ,  $\text{Rh}^{103}$ ,  $\text{I}^{127}$ ,  $\text{Sm}^{149}$ ,  $\text{Au}^{197}$  and  $\text{Hg}^{199}$  nuclei capturing thermal neutrons. It is shown that the detected gamma lines which lie in the 50–500 kev energy range can be ascribed to transitions from the lowest excited states of the investigated nuclei.

DURING THE LAST FEW YEARS many investigations were made of gamma rays emitted by nuclei in the capture of thermal neutrons. Particularly valuable measurements were made with magnetic spectrometers by two independent groups of scientists in the U.S.S.R.<sup>1</sup> and Canada<sup>2</sup>. Both groups obtained similar results. However, the softest gamma rays emitted in the  $(n, \gamma)$  reaction have not been studied extensively. The energy data for soft-gamma lines given by previous experimenters<sup>3-5</sup> require remeasurement; the intensity of the soft gamma quanta have not been determined.

In the present work a single crystal luminescent spectrometer was used to measure the energy and the absolute yields of gamma quanta in the energy interval of 50–500 kev, emitted by nuclei in the capture of thermal neutrons. Several preliminary results have been reported previously<sup>6</sup>.

### 1. EXPERIMENTAL GEOMETRY AND LUMINESCENT SPECTROMETER

An experimental physical heavy water reactor<sup>7</sup> was used as a neutron source. A neutron collimator consisting of thick layers of  $\text{B}_4\text{C}$  and Pb was placed in a horizontal channel within the reactor shield. A 12 cm thick Bi shield to prevent the gamma rays from the reactor from entering the collimation channel was affixed close to the reactor vessel. The intensity of the collimated beam of thermal neutrons brought out of the reactor was  $\sim 10^7$  neutrons/cm<sup>2</sup> sec.

The geometry of the experiment is shown in Fig. 1. In most of the experiments target 1 had the shape of an ellipse with semiaxes  $a = 18$  mm and  $b = 10$  mm. It was placed on an aluminum stand at an angle  $\alpha$  relative to the neutron beam. The target

was placed above a duct 3 in the lead which was used as a collimator of gamma rays (the length of the duct was 75 mm and its diameter 10 and 15 mm). To protect the  $\text{NaI}(\text{Tl})$  crystal 4 from thermal neutrons scattered from the target, the opening aperture of the gamma ray collimator was covered by  $\text{B}_4\text{C}$  2 0.3 g/cm<sup>2</sup> thick. In the experiments with Co, Rh and Au metallic targets were used. In the studies of powdered materials, such material was contained within aluminum foil .07 mm thick. The aluminum foil did not emit an observable intensity of gamma rays when placed in the neutron beam.

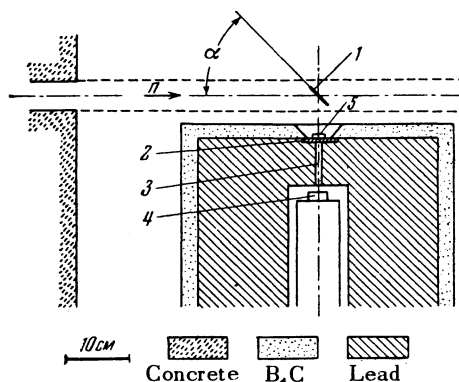


FIG. 1. Diagram of the apparatus: 1 – target, 2 –  $\text{B}_4\text{C}$  shield, 3 –  $\gamma$ -ray collimation channel, 4 –  $\text{NaI}(\text{Tl})$  crystal, 5 – lead filter.

The luminescent spectrometer employed a type S photoelectric multiplier and a  $\text{NaI}(\text{Tl})$  crystal of cylindrical shape 9 mm thick and 28 mm in diameter. The crystal was packed in a reflector made of  $\text{MgO}$ . The pulses from the photo multiplier tube had an amplitude 0.5 V and were amplified to 100 V and analyzed by a single channel amplitude analyzer with dead time of  $3 \mu\text{sec}$ .

The spectrometer characteristics (resolution, the line shape and the absolute efficiency) were studied as a function of  $\gamma$ -quanta energy by measurements on  $\text{Mo}^{99}$ ,  $\text{Hg}^{203}$ ,  $\text{B}^{10}(n, \alpha)$   $\text{Li}^{7*}$ ,  $\text{Cu}^{64}$ ,  $\text{Cs}^{137}$ , and  $\text{Zn}^{65}$ . The geometry of these measurements was similar to that in measurements of the energy and intensity of  $\gamma$ -rays in the  $(n, \gamma)$  reaction. The dependence of the resolution of the spectrometer  $\eta$  on the energy of the  $\gamma$ -rays  $E_\gamma$  is shown in Fig. 2. Fig. 3 shows the spectrum of pulses from  $\gamma$ -rays emitted in the  $\text{B}^{10}(n, \alpha)$   $\text{Li}^{7*}$  reaction (the target in the neutron beam was made of  $\text{B}_4\text{C}$ ). A photopeak for  $\gamma$ -rays at 482 kev (peak 1) is particularly clearly evident. This peak corresponds to the maximum energy distribution of Compton electrons, while peaks 2 originates in the apparatus and are due to  $\gamma$ -rays passing through the  $\text{NaI}(\text{Tl})$  crystal and scattered back in the apparatus. Peak 3 is due to the characteristic emission of lead and thus also due to the apparatus. Analogous spectra were obtained with other sources of  $\gamma$ -rays, but the position

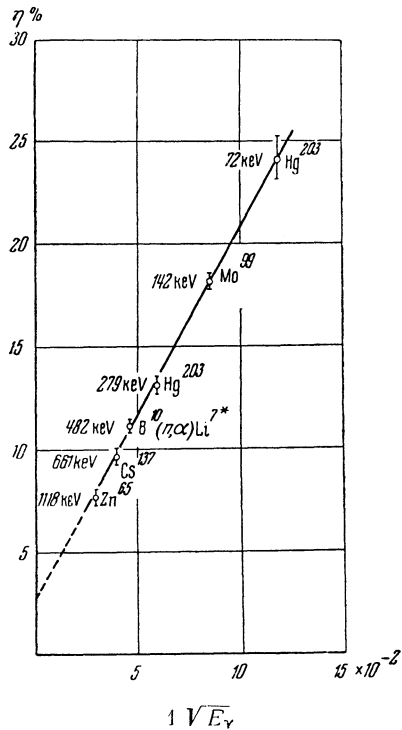


FIG. 2. Dependence of spectrometer resolving power  $\eta$  (in %) on the energy of the  $\gamma$ -rays ( $E_\gamma$  is in kev).

and the relative height of the peaks 1, 2, 3 and also of the photopeak were substantially dependent on the  $\gamma$ -ray energy. Graphs prepared from the experimental data allowed determination of the remain-

ing part of the spectra from the position of the photopeak. As a result it turned out to be possible to interpret the complex spectrum of pulses generated by the  $\gamma$ -rays, by separating parts of the spectra related to individual gamma lines. The area of the photopeak  $S_p$  was determined most accurately. By a photopeak in a spectrum of monochromatic  $\gamma$ -rays we understand a peak whose position corresponds to pulses of maximum amplitude (cf. Fig. 3).

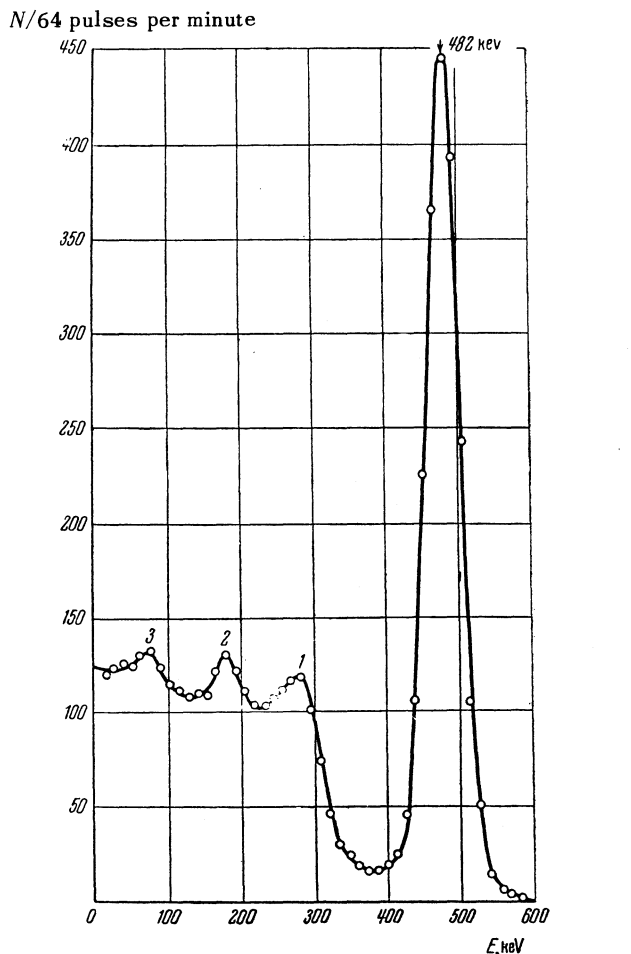


FIG. 3. Gamma ray spectrum for reaction  $\text{B}^{10}(n, \alpha)\text{Li}^{7*}$

We introduce the absolute efficiency  $\varepsilon_p$  of the spectrometer for photopeaks:

$$\varepsilon_p = \frac{S_p}{S_t} (1 - e^{-\mu x}) \quad (1)$$

where  $\mu$  is the absorption coefficient of  $\gamma$ -rays in the crystal  $\text{NaI}(\text{Tl})$ ,  $x$  is the thickness of the crystal,  $S_t$  is the total area of the spectrum of pulses,  $S_t = S_p + S_C + S_{em}$  ( $S_p$  is the area of the photopeak,

$S_C$  is the area of the Compton distribution, and  $S_{em}$  is the area of the peak due to the emission of iodine X-rays from NaI(Tl) crystal). The experimental values of the ratio  $S_p/S_t$  were found as functions of the energy of the  $\gamma$ -rays (Curve 2, Fig. 4). For the sake of comparison, Curve 1 shows the energy dependence of the ratio  $\sigma_p/(\sigma_p + \sigma_c)$  for the NaI crystal ( $\sigma_p$  and  $\sigma_c$  are the cross-sections of photoelectric absorption and Compton scattering of the  $\gamma$ -rays). The discrepancy between Curves 1 and 2 is explained by absorption of the secondary  $\gamma$  emission in the NaI crystal, which is due to the Compton scattering in the crystal. For  $\gamma$ -rays of energy  $E_\gamma < 100$  kev one notices the effect of the emission of X-rays from the crystal. The efficiency of the spectrometer  $\epsilon_p$  (Curve 3, Fig. 4) is determined from Eq. (1) taking into account the experimental Curve 2. The spectrometer is only slightly sensitive to hard  $\gamma$ -rays and it can be used for measurements of soft  $\gamma$ -rays of  $E_\gamma < 500$  kev even in the presence of the harder  $\gamma$ -lines.

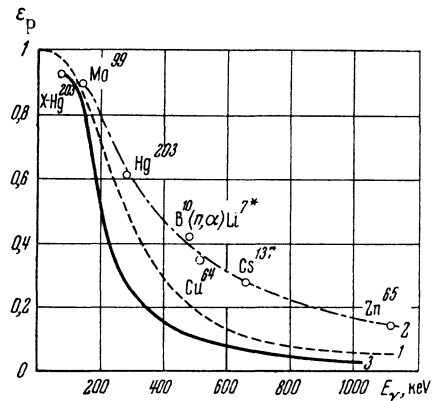


FIG. 4. Spectrometer efficiency as a function of the  $\gamma$ -quanta energy. 1 — dependence of the ratio  $\sigma_p/\sigma_p + \sigma_c$  on  $E_\gamma$ ; 2 — the experimental values of the ratio  $S_p/S_{tot}$ ; 3 —  $\epsilon_p$ .

## 2. METHOD OF MEASUREMENT OF $\gamma$ -SPECTRA

The spectrum of pulses observed in the presence of a target in the neutron beam was measured with an open beam of neutrons ( $N_0$ ) and with beam covered at the exit of neutron collimator (Fig. 1) by a layer of  $B_4C$  0.3 g/cm<sup>2</sup> thick ( $N_1$ ). The foil of  $B_4C$  absorbed thermal neutrons but did not change the flux of fast neutrons and  $\gamma$ -quanta.  $N_1$  did not depend on the presence of the target. The effect of thermal neutrons corresponds to the difference in the readings  $N = N_0 - N_1$ . In the absence of a target,  $N$  was very small. In the great majority of experi-

ments with a target, the integral count did not exceed 2,500 pulse/sec with  $N_1 \sim 700$  pulse/sec. When the beam of neutrons was obstructed by a thick layer of  $B_4C$  which absorbed both thermal and fast neutrons, the counting rate dropped to 300 pulse/sec.

Thin targets were used during the experiments since in measurements carried out with thick targets, the photopeaks were considerably wider due to the Compton scattering of the  $\gamma$ -quanta in the target. In several cases the photopeaks were somewhat wider because of slight instability of the spectrometer. As an example of the distribution of pulses in the counts of  $N_0$  and  $N_1$ , the results of measurements with  $Co_2O_3$  target are shown in Fig. 5. Curve 1 shows the spectrum of pulses with an open beam of neutrons ( $N_0$ ), Curve 2 shows the results with the same neutron beam but shielded with a  $B_4C$  foil ( $N_1$ ), Curve 3 shows the net effect of the thermal neutrons ( $N$ ). The spectrum of pulses measured in the open beam of neutrons shows peaks at 40–60 and 140 kev and a slight rise at 480 kev due to the emission from the boron shield of the spectrometer. The presence of peaks in Curve 2 makes it somewhat difficult to detect the low-intensity  $\gamma$ -lines in the regions of these peaks. The maximum at 140 kev is interpreted as absorption of neutrons in the NaI(Tl) crystal [ $\gamma$ -rays of the  $I(n, \gamma)$  reaction<sup>6</sup>]. The smeared out maximum at 450 to 550 kev, seen in Fig. 5 in the spectrum of  $\gamma$ -rays from neutron capture by the target nuclei is primarily due to  $\gamma$ -emission from the boron shield and annihilation emission.

The target both absorbed thermal neutrons and scattered them. In a control experiment, it was shown that in measurements carried out with  $B_4C$  in the  $\gamma$ -ray collimator (2 in Fig. 1) the correction for neutrons scattered by thin targets used in this work was negligible in comparison with the effect of thermal neutrons captured in the target.

Photopeaks of soft  $\gamma$ -lines appeared on a "base" of pulses caused by hard  $\gamma$ -quanta. This fact limited the accuracy in the determination of the area of the photopeak in an effort to measure the absolute number of the  $\gamma$ -quanta. To decrease the above-mentioned "base" and to separate more clearly the apparatus peaks and photopeak from  $\gamma$ -quanta emitted from the target, measurements with lead filters 0.532 – 2.55 g/cm<sup>2</sup> thick were carried out. The filters were placed in the  $\gamma$ -ray collimator. Fig. 6 shows the results of such measurements with Sm. Curve 1 represents the pulse distribution in the measurement without a lead filter, while Curve 2 shows the measurements with a 2.02 g/cm<sup>2</sup>

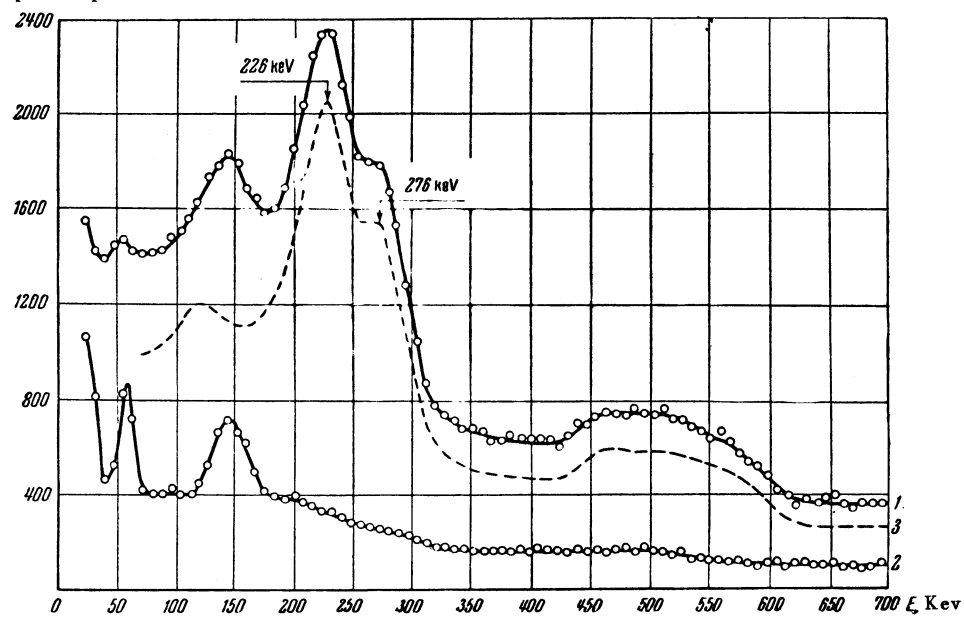
*N/64 pulses per minute*

FIG. 5. Spectrum of pulses from  $\text{Co}_2\text{O}_3$ : 1 — neutron beam open ( $N_0$ ), 2 — neutron beam covered by  $\text{B}_4\text{C}$  ( $N_1$ ), 3 — effect of thermal neutrons  $N = N_0 - N_1$ .

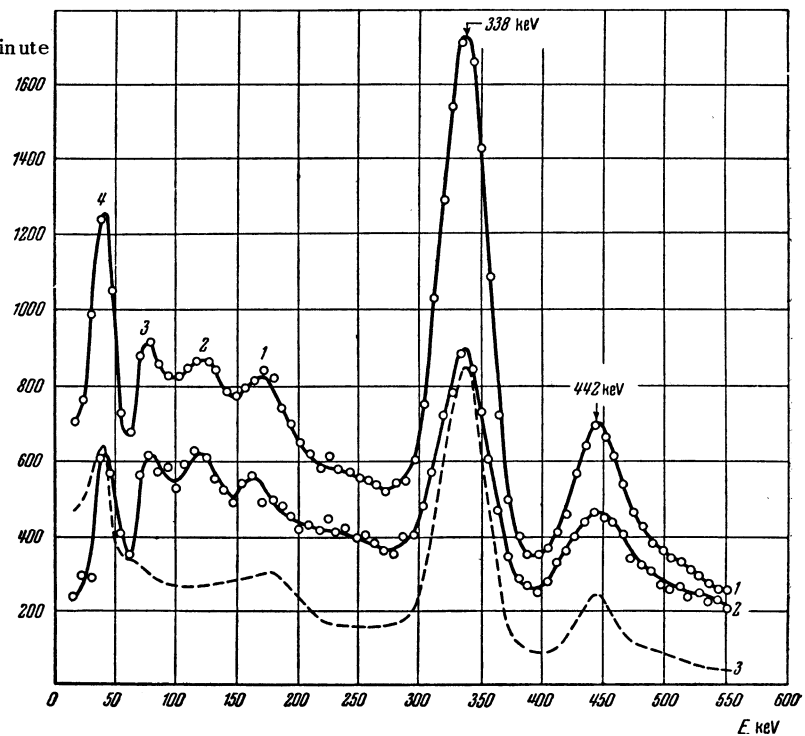
*N/64 pulses per minute*

FIG. 6. Spectrum of pulses of  $\text{Sm}^{149}(n, \gamma)\text{Sm}^{150}$   $\gamma$ -rays: 1 — without lead filter; 2 — with  $2.02 \text{ g/cm}^2$  lead filter; 3 — spectrum of pulses due to radiation absorbed in the lead filter.

lead filter. The areas of the photopeaks due to the 442 and 338 kev  $\gamma$ -quanta decrease in the measurements with lead filters, corresponding to absorption of the  $\gamma$ -rays emitted by the target. Peaks 2 and 3 do not disappear in the measurements carried out with a filter and therefore cannot be interpreted as photopeaks due to soft  $\gamma$ -quanta from the target, but appear to be due to the apparatus. Thus, peak 3 is caused by the X-rays from the spectrometer lead shield (*cf.* also Fig. 3) and peak 2 is caused by the  $\gamma$ -rays from the  $I(n, \gamma)$  reaction within the NaI(Tl) crystal. The origin of the peaks 1 and 4 will be discussed below (Sec. 3, *Samarium*). In reducing the results of the measurements, the pulse spectra of  $\gamma$ -rays absorbed in the lead filters were utilized (Curve 3).

Measurement of the area of the photopeak  $S_p$  alone is not sufficient to determine the number of  $\gamma$ -quanta emitted in the capture of neutrons by the target. To determine this quantity it is necessary to know the solid angle subtended by the target at the NaI(Tl) crystal and the neutron flux. Independent determinations of these quantities would serve as a source of additional errors. In an effort to obviate such errors in the present work, the area of the sought photopeaks  $S_p^i$  was compared with the area of the photopeak due to the 482 kev  $\gamma$ -quanta  $S_p^B$  which was determined in measurements with a  $B_4C$  target in an identical manner as with the target made of the studied material. The  $B_4C$  target was placed in the beam of thermal neutrons in place of the target prepared from the investigated isotope and its thickness was such that the absorption of thermal neutrons was almost complete. Then

$$\frac{S_p^i}{S_p^B} = \frac{n_{\gamma i}}{n_{482}} \frac{\epsilon_p^i}{\epsilon_p^{482}} \frac{k_i}{k_{482}} \sigma_{\text{capt}} \frac{pL}{A} \alpha. \quad (2)$$

In Eq. (2)  $n_{\gamma i}$  is the unknown number of  $\gamma$ -quanta emitted per single captured neutron,  $n_{482}$  is the same number for  $B^{10}(n, \alpha) Li^{7*}$  ( $n_{482} = .93$ ),  $k_i$  and  $k_{482}$  are correction factors for the absorption of  $\gamma$ -quanta in the path from the target to the NaI(Tl) crystal. The quantity  $\sigma_{\text{capt}} pN_0/A$  is the probability of the neutron capture by the target nuclei ( $\sigma_{\text{capt}}$  is the neutron capture cross-section,  $p$  is the mass of the target,  $L$  is the Avogadro's number, and  $A$  is the molecular weight). The factor  $\alpha$  takes into account the absorption of neutrons and  $\gamma$ -quanta in a target of thickness  $l$ :

$$\alpha = \frac{1 - \exp \{ - (\mu_n + \mu_\gamma \tan \alpha) l / \sin \alpha \}}{(\mu_n + \mu_\gamma \tan \alpha) l / \sin \alpha}, \quad (3)$$

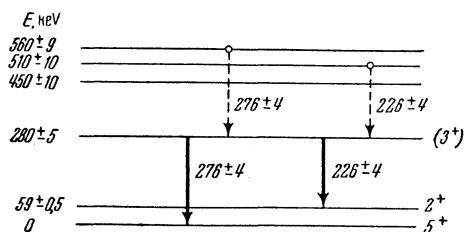
where  $\mu_n$  and  $\mu_\gamma$  are the absorption coefficients of neutrons and  $\gamma$ -quanta, and  $\alpha$  is the angle at which the target is oriented relative to the direction of neutron beam (Fig. 1). In the calculations of  $\alpha$ , the values of  $\mu_\gamma$  were taken from the work of Davisson and Evans<sup>8</sup>.

### 3. RESULTS OF MEASUREMENTS

#### Cobalt

In the measurements on cobalt the target was prepared of powdered cobalt oxide (6.94 g) and metal (2.21 g). The powdered cobalt oxide was packed in a cylindrical case made of aluminum foil. The metallic target had an elliptical shape. From the known contents of impurities in the targets it was concluded that the  $\gamma$ -rays due to neutron capture in the target are practically entirely due to capture by  $Co^{60}$ . In the pulse spectrum from the  $Co_2O_3$  target (Fig. 5) there are two not fully resolved peaks of energies  $226 \pm 4$  and  $276 \pm 4$  kev, which are interpreted as photopeaks due to  $\gamma$ -quanta of the same energies. The possibility of the presence of peaks due to  $\gamma$ -rays from cobalt with the intensity of the order of several percent in the 450–550 kev energy range cannot be excluded. The small peak at 120 kev was shown by additional experiments on absorption of  $\gamma$ -rays in lead filters to originate in the apparatus. Four independent series of measurements were carried out on the  $\gamma$ -ray spectra of cobalt absorbed by lead filter 2.02 g/cm<sup>2</sup> thick: two with a cobalt oxide target and two with a metallic target. These measurements were combined with the measurements of the area of the photopeak from a  $B_4C$  target. The resultant intensities of the  $\gamma$ -lines were found to be  $n_{226} = (23 \pm 4)\%$  and  $n_{276} = (23 \pm 4)\%$ . The effective cross-section for capture of thermal neutrons in cobalt was taken to be 35.4 barns.

The values of the  $\gamma$ -transition energies obtained in the present work are close to the results of Hamermesh and Hummel<sup>3</sup> (220 kev) and agree with the results of Reier and Shamos<sup>4</sup> (237 and 289 kev). In these experiments the  $\gamma$ -rays from the  $Co(n, \gamma)$  reaction were measured by luminescent spectrometers. From measurements of hard  $\gamma$ -rays of the  $Co(n, \gamma)$  reaction<sup>9</sup> and the energies of proton groups in the  $Co(d, p)$  reaction<sup>10</sup> the energies of the excited levels of  $Co^{60}$  nucleus were determined and found to be in good agreement with each other. The lowest of these energies are shown in Fig. 7 together with the  $\gamma$ -transitions whose energies are

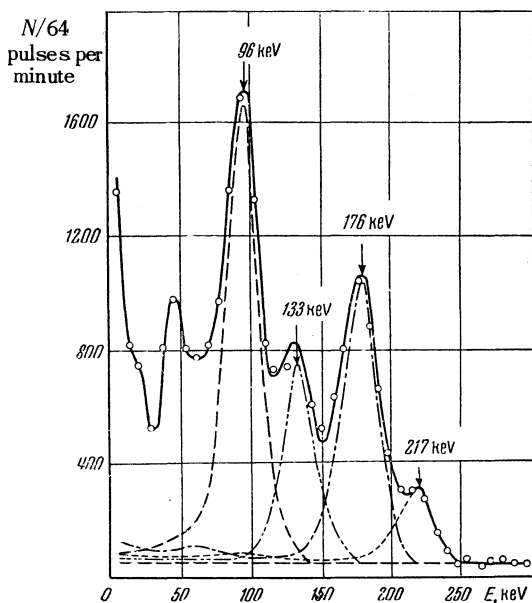
FIG. 7. Lowest energy levels of  $\text{Co}^{60}$ .

close to the energies of the  $\gamma$  lines measured in our experiment. It is possible to have either a combination of the shown transitions with transitions between several high-energy levels of the excited nucleus with various relative intensities, or their individual combinations. The case of a cascade transition containing only one of the pair of  $\gamma$ -rays of energies 280 and 220–230 kev is highly unlikely. Indeed, for  $n_{226} = n_{276}$  the transitions of cascades from higher levels to the intermediate levels would have to be considered in this case as forbidden without any reasons for such an assumption. Because of the comparatively high intensity of the  $\gamma$ -lines observed by us, it is most probable that the transitions corresponding to these lines take place between the lowest levels of  $\text{Co}^{60}$ , i.e., from the 200 kev level to the ground and isomeric levels, and that the remaining possible transitions of similar energies introduce only a small contribution to the intensities  $n_{226}$  and  $n_{276}$  (such an assumption is not in a contradiction with the values of the activation cross sections for the ground and isomeric states of  $\text{Co}^{60}$ ). In this case it is possible to make several assumptions about the characteristics of the 280 kev energy level. In consequence of the equality of transition probabilities from the 280 kev energy level to the isomeric and ground levels, it is possible to assume that the angular momentum of the 280 kev level is equal to either 3 or 4, since the characteristics of the ground and isomeric levels are  $5^+$  and  $2^+$ , respectively<sup>11</sup>. A comparison of the data reported previously<sup>9,10</sup> results in the conclusion that there are no transitions from the initial state of  $\text{Co}^{60}$  (which is formed after the capture of thermal neutrons by  $\text{Co}^{59}$ ) to the isomeric level. This fact shows that the initial state of  $\text{Co}^{60}$  has a characteristic  $4^-$  and not  $3^-$  (the ground state of  $\text{Co}^{59}$  has a characteristic  $7/2^-$ ).<sup>12</sup> The transitions from the initial state of  $\text{Co}^{60}$  to the ground state and to the 280 kev energy level have approximately the same intensity, namely 3 and 4% respectively<sup>9</sup>. Since the transition to the ground state is  $E1$ , then the transition to the 280 kev energy level

should also be  $E1$ , i.e., the parity of this level is positive. From the two possible values of the angular momentum for the 280 kev energy level the most preferred value is  $l = 3$ . In this case the transition to the isomeric level with lower energy should be  $M1$  and the higher energy transition to the ground state should be  $E2$ .

### Rhodium

A metallic plate of elliptical shape 0.1 mm thick and weighing 0.669 grams was used as a target for experiments on rhodium. Rhodium has one stable isotope  $\text{Rh}^{103}$ , so that the  $\gamma$ -rays of the radiative neutron capture belong to  $\text{Rh}^{104}$ . In this experiment the energy range up to 300 kev was studied in detail. Fig. 8 shows the pulse spectrum of  $\gamma$ -rays absorbed by a  $1.01 \text{ g/cm}^2$  lead filter. The separation of this spectrum into the individual components, shown in the figure by dotted lines made possible a determination of the areas of those photopeaks for which the experiments on absorption of  $\gamma$ -rays reliably show their origin to be in the target. An analogous technique was used for the pulse spectrum of  $\gamma$ -rays absorbed by a  $0.532 \text{ g/cm}^2$  filter. The energies and absolute intensities of  $\gamma$ -lines were found to be:  $E_1 = 96 \pm 3$ ,  $E_2 = 133 \pm 3$ ,  $E_3 = 176 \pm 3$ ,  $E_4 = 217 \pm 4$  kev and similarly  $n_1 = 17\%$ ,  $n_2 \leq 8\%$ ,  $n_3 = 19\%$ ,  $n_4 = 9\%$ . The effective cross-section for capture of thermal neutrons

FIG. 8. Spectrum of pulses due to  $\gamma$ -rays from  $\text{Rh}(n, \gamma)$  reaction, absorbed by lead filter  $1.01 \text{ g/cm}^2$  thick.

in rhodium was taken to be 150 barns. The errors in the determination of  $n_1 - n_4$  are 15 to 20%. For the 133 kev line only the upper limit of intensity is shown since in that energy range there is a background peak (Fig. 5), which is not entirely eliminated in the difference of readings with open and closed neutron beams. The energy peak at 45 kev did not disappear in measurements with lead filters and consequently was due to the equipment.

It was observed previously<sup>6</sup> that the 80 and 160 kev  $\gamma$ -quanta discovered by Hamermesh and Hummel<sup>3</sup> in the  $\gamma$ -ray spectrum of radiative capture of neutrons in rhodium apparently correspond to the most intense  $\gamma$ -lines measured in the present work. The measurements of the hard  $\gamma$ -rays in the  $\text{Rh}(n, \gamma)$  reaction carried out previously<sup>13</sup> permit determinations of the energies of the lower levels of the  $\text{Rh}^{104}$  nucleus. The characteristics of the ground and the first two excited levels are determined from the  $\beta$ -decay of  $\text{Rh}^{104}$ <sup>14</sup>. It should be noted that only for  $0^-$ , the characteristics of the initial state of  $\text{Rh}^{104}$ , produced by absorption of thermal neutrons by  $\text{Rh}^{103}$ , and  $2^+$  of the first excited level, is it possible to explain the absence of transitions from the initial level to the first excited level<sup>13</sup>. The principles which were used in Ref. 13 to assume  $I = 1$  for the ground state should be reevaluated.

The energies of  $\gamma$ -lines found in this work do not fit directly into the energy level scheme constructed from the data of previous experiments<sup>13, 14</sup> (Fig. 9, solid lines). If the presence of an additional 230 kev level is assumed, then these  $\gamma$ -lines are distributed in the scheme as shown by the dotted line in Fig. 9. In this case, however, there is a discrepancy between the intensity of the 96 kev  $\gamma$ -transition to the isomeric level ( $17 \pm 3\%$ ) and the probability of activation of the 4.3 minute isomer  $\text{Rh}^{104}$  ( $8 \pm 3\%$ ). This discrepancy exceeds the experimental error. Furthermore, it is difficult to reconcile the approximately equal intensities of the 96 and 176 kev  $\gamma$ -lines with the values of the radiative transition probabilities for the values of the angular momenta and parities of the first and the second excited levels of  $\text{Rh}^{104}$  shown in Fig. 9. At the most suitable characteristics of the introduced level ( $3^-$ ), transitions with these energies will be  $E2$  and  $M2$ , respectively. The ratio of the transition probabilities calculated by the Weisskopf formula<sup>15</sup> is approximately 5. A satisfactory arrangement of the energies of the observed  $\gamma$ -lines in the energy level scheme of  $\text{Rh}^{104}$  can be accomplished by introducing two additional levels. How-

ever, the possible energies of these levels cannot be determined uniquely.

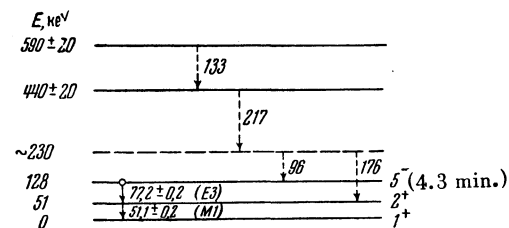


FIG. 9. Energy levels of  $\text{Rh}^{104}$ .

### Iodine

A target of powdered iodine (3.96 g) was used. The  $\gamma$ -ray pulse spectrum of the  $\text{I}^{127}(n, \gamma)\text{I}^{128}$  reaction showed an intense  $135 \pm 3$  kev  $\gamma$ -line<sup>6</sup>. Existence of low-intensity  $\gamma$ -lines in the 255 kev energy range is possible<sup>4</sup>. The discrepancy with the data of Reier and Shamos<sup>4</sup> can apparently be explained by the fact that no shielding of the NaI(Tl) crystal from neutrons scattered by the target was used in the luminescent spectrometer. It is important to note that the scattering cross section of neutrons by iodine is approximately equal to the capture cross-section. In the measurements with any target carried out without  $\text{B}_4\text{C}$  in the  $\gamma$ -ray collimator (2 in Fig. 1) peaks at energies 85, 135 and 255 kev were observed. It is probable that for this reason the  $\gamma$ -quanta of 135 kev energy were attributed by the authors of the above work to background noise while the 80 kev peak they attributed erroneously to  $\gamma$ -rays from the  $\text{I}(n, \gamma)$  reaction.

From twelve distinct series of measurements, which included six measurements of  $\gamma$ -ray spectra using a lead filter, the intensity of 135-kev  $\gamma$ -lines was determined with an accuracy of 15%. This intensity is  $n = 32\%$  per single captured neutron. The capture cross section in iodine was taken to be 6.7 barns. The absence of other intense  $\gamma$ -lines in the energy range up to 600 kev and the great intensity of  $\gamma$ -quanta of energy 135 kev shows that these  $\gamma$ -quanta are indeed connected with a transition from the first excited level of  $\text{I}^{128}$  to the ground state.

### Samarium

The target in the experiments on samarium was powdered  $\text{Sm}_2\text{O}_3$  (76.5 mg), packed in an aluminum foil case in the shape of a disk 10 mm in diameter.

The spectrum of pulses from the samarium target is shown in Fig. 6. Two well resolved peaks of  $\gamma$ -quanta at energies  $442 \pm 5$  and  $338 \pm 4$  kev are clearly visible in the pulse spectrum of  $\gamma$ -rays absorbed by a lead filter (Curve 3). A smaller maximum appearing as a decrease in peak I in measurements with a lead filter was interpreted as the maximum of the Compton distribution of electrons from  $\gamma$ -quanta of 338 kev energy. The origin of peaks 2 and 3 was discussed in Sec. 2. The energy of peak 4 corresponds to the X-ray emission from Sm within the experimental accuracy. However, an intense peak due to the experimental equipment is observed in the spectrum at the same energy and its presence makes it impossible to measure the X-ray emission of Sm when its intensity is less than 10%. Thus,  $\gamma$ -lines of observable intensities are absent at energies below 300 kev. From the experiments the intensities of the observed  $\gamma$ -lines were determined to be  $(34 \pm 5)\%$  ( $E_\gamma = 442$  kev) and  $(70 \pm 10)\%$  ( $E_\gamma = 338$  kev) per single captured neutron. The capture cross section of neutron by the Sm<sup>149</sup> isotope was taken to be 66,200 barns<sup>17</sup>. This result depends only very slightly on the error in the determination of the cross section since the target absorbed almost all the thermal neutrons incident on it. The energies of the  $\gamma$ -lines are in excellent agreement with the data of other authors<sup>5,16</sup> who studied the spectra of  $\gamma$ -rays in the Sm( $n, \gamma$ ) reaction, while the intensity of the  $\gamma$ -line at 338 kev is approximately twice the intensity found by Adiasevich *et al.*<sup>16</sup>. The  $\gamma$ -lines investigated should be attributed to transitions to two lowest excited levels of Sm<sup>150</sup>, since the major contribution to the cross section for capture of thermal neutrons in the existing composition of Samarium isotopes is due to Sm<sup>149</sup>. The fact that the discussed levels appear in the decay of Pm<sup>150</sup><sup>18</sup> adds to the likelihood of such an assumption. From the relationship of the  $\gamma$ -line intensities it follows that the first excited level of Sm<sup>150</sup> is the energy level at  $338 \pm 4$  kev. This conclusion is in agreement with the data of Ref. 18. The second excited level has an energy 777 kev<sup>5,19</sup>. The low intensity of hard  $\gamma$ -lines in the spectrum of Sm( $n, \gamma$ )<sup>16,19</sup> shows that the radiative transition of the Sm<sup>150</sup> nucleus from the state originating by capture of a thermal neutron takes place through cascade  $\gamma$ -transitions which result with equal probability in a ground state or in one of the two above levels of Sm<sup>150</sup>. The decay scheme of Sm<sup>150</sup> proposed previously<sup>16</sup> thus appears to be incomplete.

### Gold

The measurements for gold were carried out with two metallic targets of pure gold: I - 0.277 g/cm<sup>2</sup> thick, (1.56 g) and II - 0.554 g/cm<sup>2</sup> thick. Figure 10 shows the pulse spectrum of  $\gamma$ -quanta absorbed in a 2.02 g/cm<sup>2</sup> lead filter. In this diagram one can identify three not fully resolved photopeaks whose energies are 252, 210 and 174 kev (target II). The accuracy of the energy determination was  $\pm 4$  kev. In separating the spectrum into the individual components (the dotted lines of Fig. 10) a small remaining contribution in the energy region of about 140 kev is probably due to the background noise (cf. Fig. 5). Table I gives the intensities  $n_\gamma$  of the observed  $\gamma$ -lines measured with an accuracy of  $\pm 20\%$ . The capture cross section of thermal neutrons was taken to be 98 barns<sup>20</sup>.

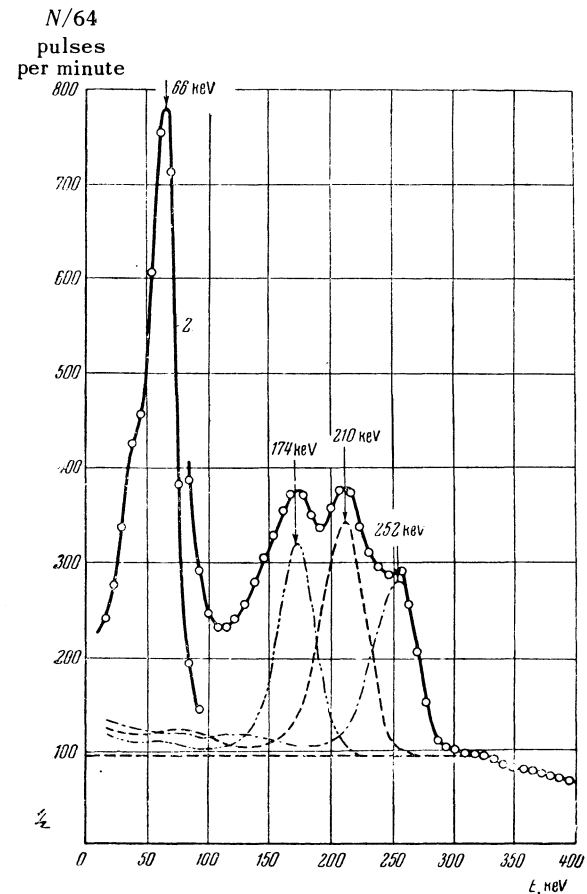


FIG. 10 Spectrum of pulses due to Au( $n, \gamma$ )  $\gamma$ -rays absorbed in 2.02 g/cm<sup>2</sup> lead filter.

Besides the photopeaks mentioned above, an additional maximum at  $66 \pm 3$  kev is clearly evident in Fig. 10. This maximum is also due to the capture

of neutrons in gold. The thin target (*I*) was used in the measurements of the intensity of this emission. The absorption of  $\gamma$ -quanta in the target was determined experimentally. Gold plates were used instead of lead filters 5 of Fig. 1 and the absorption

was determined from the decrease in the area of the peak. In this way the coefficient of  $\gamma$  absorption  $66 \pm 3$  kev  $\gamma$ -quanta in Au was determined to be  $\mu = 2.9 \pm .2$   $\text{cm}^2/\text{g}$ . The intensity of the considered radiation is shown in Table I.

TABLE I. Soft  $\gamma$ -quanta of Au ( $n, \gamma$ ) reaction

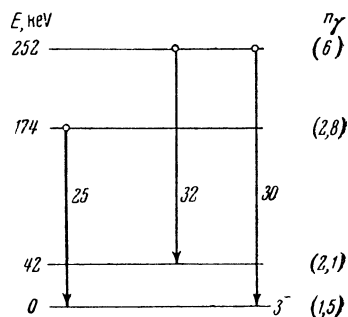
| $E$ in kev | No. of $\gamma$ -quanta per single captured neutron % | Theoretical values of internal conversion coefficient $a_K$ in K shell |       |      |
|------------|---|--|-------|------|
|            |   | $E2$   | $M1$  | $M2$ |
| 252        | 22  | 0.0955   | 0.447 | 1.66 |
| 210        | 19  | 0.152  | 0.775 | 3.47 |
| 174        | 11  | 0.278  | 1.47  | 7.42 |
| 66         | 40  | —  | —     | —    |

Reier and Shamos<sup>4</sup> discovered 248-kev  $\gamma$ -lines in the spectrum of Au( $n, \gamma$ ), which correspond apparently to a summary peak composed of the three  $\gamma$ -lines disclosed in the present work. From an experimental point of view the conclusions of Bartholomew and Kinsey<sup>13</sup> that the neutron binding energy in Au<sup>198</sup> exceeds 6.5 Mev are hardly conclusive. A similar doubt has also been expressed previously<sup>4</sup>. It is more likely, in agreement with London and Saylor<sup>21</sup>, that the  $6.494 \pm .008$  Mev  $\gamma$ -quanta are due to direct transition of the nucleus into the ground state. Then the lowest excited states of Au<sup>198</sup> (from the data of Ref. 13) have excitation energies  $32 \pm 20$ ,  $184 \pm 16$ ,  $245 \pm 17$ ,  $348 \pm 20$ ,  $518 \pm 20$ , and  $792 \pm 20$  kev. The  $\gamma$ -lines discovered in the present work can be interpreted as due to transitions between the lowest levels of Au<sup>198</sup> (Fig. 11). At the same time the 210-kev

the more probable. In our measurements, the 42-kev  $\gamma$ -rays were not observed because of strong absorption in the target and the presence of a neighboring background peak (cf. Fig. 5).

The  $66 \pm 3$  kev gamma quanta cannot be reconciled with any transition between the lowest excited states. This emission was interpreted as X-ray emission from Au and due to internal conversion of  $\gamma$ -quanta in the K shell of the atom. Taking into account the K fluorescence from Au ( $f = 0.94$ )<sup>22</sup> we find the number of conversions in the K shell to be  $K = 42 \pm 6\%$  per captured neutron. It is not possible in our work to attribute the X-rays to conversion of a soft line that cannot be detected because of its low intensity. Such an explanation is impossible since one would have to allow a complete conversion of such hypothetical line and the Au<sup>198</sup> nucleus does not have a metastable state. It is most likely that the conversion is connected with the  $\gamma$ -quanta detected in this work:  $K = K_{252} + K_{210} + K_{174}$ . Table I gives the theoretical values of the coefficients  $a_K$  of the internal conversion of  $\gamma$ -rays by the K shell electrons of Au for dipole and quadrupole transitions<sup>23</sup>. The higher multipoles do not enter because of the long lifetime. The gamma-quanta intensity  $n_\gamma$  found in this work permits the use of  $a_K$  to determine the number  $K$  of conversion events in the K shell of the atom, which depends on the multipole order of all three  $\gamma$ -lines. The multipole orders of the  $\gamma$ -transitions were so chosen as to satisfy the experimental values of  $K$ .

The experimental results exclude the possibility that all three transitions are of the  $E2$  type ( $K = 7.6 \pm 1.5$ ) or  $M2$  ( $K = 161 \pm 30$ ). If the  $\gamma$ -transition of 252 kev energy is attributed to  $M2$ , and the other two transitions to  $M1$  or  $E2$ , then one

FIG. 11. Transition scheme for Au<sup>198</sup>.

$\gamma$ -quanta of energy cannot be considered as due to a transition between any one of the above levels, while the other two  $\gamma$ -quanta can correspond to transitions between somewhat higher levels. In our opinion, the transition scheme shown in Fig. 11 is

obtains a satisfactory agreement with the experimental data. However, this variant is rather improbable, since the  $M2$  transitions could not compete with  $M1$  and  $E2$  transitions in the above transition scheme (Fig. 11). A better agreement with the experiment is achieved if all three transitions are assumed to be  $M1$  ( $K = 38 \pm 8$ ). The case of two  $M1$  transitions (one of which should be the transition at 174 kev) and one  $E2$  transition is also possible. Fig. 11 shows (in percent per single captured neutron) the total number of transition events from excited states, equal to the sum of probabilities of transitions by  $\gamma$ -quantum emission (Table I), and of the transitions by conversion of  $\gamma$ -quanta conversion of atomic  $K$  electrons assuming that the transitions are of the  $M1$  type.

The  $Au^{198}$  nucleus has negative parity and spin  $I = 3$  in the ground state<sup>3</sup>. The excited levels shown in Fig. 11 should also have negative parity, since only  $M1$  or  $E2$  transitions are possible between them. According to Ref. 25, the initial state of  $Au^{198}$ , produced when  $Au^{197}$  captures a thermal neutron, has a spin  $1^+$ . Bartholomew and Kinsey<sup>13</sup>

showed that the probabilities of transitions from the initial state to the particular levels of  $Au^{198}$  considered here are of the same order of magnitude. The number of  $\gamma$ -transitions from the initial state to the state corresponding to a given energy level is shown in parentheses of Fig. 11 in percent per single captured neutron. The above facts can be brought into agreement by an assumption that the lowest excited levels have the same spin 3, even though such degeneracy seems unlikely to us. Furthermore, the transitions from the initial state to the considered levels, including the ground level, will be  $M2$  transitions, which should be suppressed by the  $E1$  and  $M1$  transitions. Here it is expedient to reconsider the conclusion of Titman and Sheer<sup>25</sup> about the spin of the initial state. The results of a later work<sup>20</sup> disagree with the data used in their work to obtain  $1^+$  for the spin and parity of the initial state. If the initial state of  $Au^{198}$  is  $2^+$ , the transitions into the considered levels will be  $E1$  and the spins and parities of the corresponding states of  $Au^{198}$  will be  $1^-$ ,  $2^-$ , and  $3^-$  for small excitation energies.

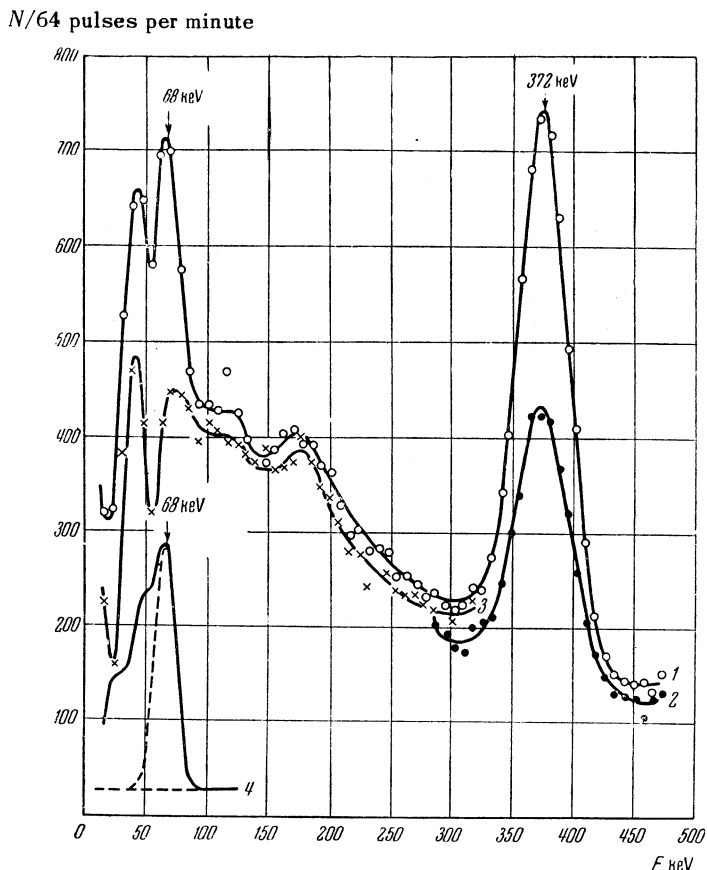


FIG. 12. Spectrum of pulses from  $\gamma$ -rays of Hg: 1 — without lead filter; 2 — with  $2.02$   $g/cm^2$  lead filter; 3 — with  $0.5$  mm lead filter; 4 — emission spectrum absorbed by  $0.5$  mm of lead.

*Mercury*

The measurements on Hg were carried out using a powdered target of HgO (1.2 g) packed in disc-shaped aluminum case 20 mm in diameter. The spectrum obtained with this target (Curve 1 Fig. 12) shows a particularly noticeable photopeak due to  $372 \pm 5$  kev  $\gamma$ -quanta. Peaks corresponding to somewhat softer radiation are also apparent. Curve 2 of Fig. 12 refers to measurements with a  $2.02 \text{ g/cm}^2$  lead filter. From the spectrum of the radiation absorbed by the lead filter (difference of Curves 1 and 2) the area of the photopeak was determined, and  $n_\gamma = 45 \pm 7\%$  per single captured neutron was obtained for the intensity of the radiation at 372 kev. The capture cross section of thermal neutrons was taken to be 380 barns. From a comparison of Curves 1 and 3 (the pulse spectrum of  $\gamma$ -rays which passed through a lead filter 0.5 mm thick) it is evident that the  $68 \pm 3$  kev radiation originates in the target, while the 45-kev peak appears to be due to the experimental apparatus. In the lower left-hand corner of Fig. 12 is shown a spectrum of radiation absorbed by 0.55 mm Pb (Curve 4). From this curve, the intensity of the  $68 \pm 3$  kev radiation was determined to be  $1.4\% < n_\gamma < 4\%$  per single captured neutron. The apparatus peak makes it difficult to establish this intensity more accurately.

The  $\gamma$ -quanta observed in these experiments

should be ascribed to Hg<sup>200</sup> since the isotope Hg<sup>199</sup> has the largest thermal neutron capture cross section of the mercury isotopes. The 372-kev  $\gamma$ -quanta correspond here to the transition of Hg<sup>200</sup> from the first excited state to the ground state, well known<sup>25</sup> from the radioactive decay of Au<sup>200</sup> and Tl<sup>200</sup>. Gamma quanta of similar energy were detected<sup>16</sup> in the study of  $\gamma$ -rays emitted after capture of neutrons in Hg, except that our measured intensity is greater by approximately a factor of two. A similar discrepancy from the above work<sup>16</sup> has appeared in our data on the intensity of the soft line of the Sm( $n, \gamma$ ) reaction.

The  $68 \pm 3$  kev radiation can naturally be interpreted as mercury X-rays and can be ascribed to 372 kev  $\gamma$ -ray conversion in the K shell of the atom. The experimental values of the internal conversion coefficient  $a_K$  in the K shell is between the limits  $0.03 < a_K < 0.09$ . A theoretical value can be found within these limits only for E2 transitions ( $a_K \sim 0.04$ )<sup>22</sup>. Consequently, the first excited state of Hg<sup>200</sup> should have spin 2 and positive parity in agreement with a previous work<sup>26</sup>.

## SUMMARY OF RESULTS

Table II gives the values of energies  $E_\gamma$  and intensities  $n_\gamma$  of the  $\gamma$ -lines (number of  $\gamma$ -quanta per single captured neutron). The absolute intensities were determined with an accuracy of  $15 \pm 20\%$ .

TABLE II.

| Emitting nucleus  | Energy $E$ of the $\gamma$ -quanta in kev | No. of $\gamma$ -quanta per single captured neutron, $n_\gamma$ , % | Emitting nucleus  | Energy $E$ of the $\gamma$ -quanta in kev | No. of $\gamma$ -quanta per single captured neutron, $n_\gamma$ , % |
|-------------------|---|---|-------------------|---|---|
| Co <sup>60</sup>  | $226 \pm 4$                               | 23  |                   |   |   |
|                   | $276 \pm 4$                               | 23  | Sm <sup>150</sup> | $338 \pm 4$                               | 70  |
| Rh <sup>104</sup> | $96 \pm 3$                                | 17  |                   | $442 \pm 5$                               | 34  |
|                   | $133 \pm 3$                               | $\leq 8$  | Au <sup>198</sup> | $66 \pm 3$                                | 40  |
|                   | $176 \pm 3$                               | 19  |                   | $174 \pm 4$                               | 11  |
|                   | $217 \pm 4$                               | 9   |                   | $210 \pm 4$                               | 19  |
| I <sup>128</sup>  | $135 \pm 3$                               | 32  |                   | $252 \pm 4$                               | 22  |
|                   |   |   | Hg <sup>200</sup> | $68 \pm 3$                                | $1.4 - 4$   |
|                   |   |   |                   | $372 \pm 5$                               | 45  |

In conclusion the authors express their gratitude to I. M. Frank for his interest in this work, I. S. Shapiro for evaluation of the results, A. M. Safronov, V. F. Tsarakev, Ia. A. Kleinman and associates, who operated the reactor, for their help in this work.

*Russian Delegation to the International Conference of Peaceful Uses of Atomic Energy*, Published by U.S.S.R. Acad. Sci., p. 252 (1955).

<sup>2</sup> B. B. Kinsey and G. A. Bartholomew, Can. Journ. Phys. **31**, 537 (1953).

<sup>3</sup> B. Hamermesh and V. Hummel, Phys. Rev. **88**, 916 (1952).

<sup>1</sup> Groshev, Adiasevich, and Demidov, *Papers by the*

- <sup>4</sup> M. Reier and M. H. Shamos, Phys. Rev. **100**, 1302 (1955).
- <sup>5</sup> C. T. Hibdon and C. D. Muehlhause, Phys. Rev. **88**, 945 (1952).
- <sup>6</sup> Estulin, Kalinkin, and Melioranskii, J. Exptl. Theoret. Phys. (U.S.S.R.) **31**, 886 (1956), Soviet Physics JETP **4**, 752 (1957).
- <sup>7</sup> Alikhanov, Vladimirkii, Nikitin, Galanin, Gavrilov, and Burgov, *Papers by the Russian Delegation to the International Conference of Peaceful Uses of Atomic Energy*, p. 105 (1955).
- <sup>8</sup> C. M. Davisson and R. D. Evans, Rev. Mod. Phys. **24**, 79 (1952).
- <sup>9</sup> G. A. Bartholomew and B. B. Kinsey, Phys. Rev. **89**, 368 (1953).
- <sup>10</sup> G. M. Foglesong and D. G. Foxwell, Phys. Rev. **96**, 1001 (1954).
- <sup>11</sup> M. Deutch and G. Scharff — Goldhaber, Phys. Rev. **83**, 1059 (1951).
- <sup>12</sup> L. K. Peker and L. A. Sliv, Izv. Akad. Nauk SSSR, Ser. Fiz. **27**, 411 (1953).
- <sup>13</sup> G. A. Bartholomew and B. B. Kinsey, Can. Journ. Phys. **31**, 1025 (1953).
- <sup>14</sup> Jordan, Cork, and Burson, Phys. Rev. **90**, 362 (1953).
- <sup>15</sup> J. M. Blatt and V. F. Weisskopf, *Theoretical Nu-*
- clear Physics* (John Wiley & Sons, New York, 1952).
- <sup>16</sup> Adiasevich, Groshev, and Demilov, U.S.S.R. Acad. Sci., *Conference on Peaceful Uses of Atomic Energy*, p. 270 (1955).
- <sup>17</sup> Melaike, Parker, Petruske, and Tomlinson, Can. Journ. Chem. **33**, 830 (1955).
- <sup>18</sup> V. Kistiakov — Fischer, Phys. Rev. **96**, 1549 (1956).
- <sup>19</sup> B. B. Kinsey and G. A. Bartholomew, Can. Journ. Phys. **31**, 1051 (1953).
- <sup>20</sup> H. H. London and V. L. Silar, Phys. Rev. **93**, 1030 (1954).
- <sup>21</sup> A. Harvey, Phys. Rev. **81**, 353 (1951).
- <sup>22</sup> Brogues, Thomas, and Haynes, Phys. Rev. **89**, 715 (1953).
- <sup>23</sup> L. A. Sliv and H. N. Brand, *Tables of Internal Conversion Coefficients*, 1956.
- <sup>24</sup> Elliot, Preston, and Wolfson, Can. Journ. Phys. **32**, 153 (1954).
- <sup>25</sup> J. Titman and C. Sheer, Phys. Rev. **83**, 747 (1953).
- <sup>26</sup> Berstrom, Hill, and de Pasquali, Phys. Rev. **92**, 918 (1953).

Translated by M. J. Stevenson  
215

SOVIET PHYSICS JETP

VOLUME 5, NUMBER 5

DECEMBER, 1957

### Ignition of the High Voltage Discharge in Hydrogen at Low Pressures

A. S. POKROVSKAIA-SOBOLEVA AND B. N. KLIARFEL'D

(Submitted to JETP editor January 14, 1957)

J. Exptl. Theoret. Phys. (U.S.S.R.) **32**, 993-1000 (May, 1957)

It has been found that the striking voltages for discharges in hydrogen, corresponding to the left-hand branch of the Paschen curve, do not obey the similarity rules.

After an ignition on the left-hand branch of the Paschen curve, the resultant high-voltage discharge is characterized by electrode voltage drops which are independent of the current. In hydrogen discharges, this constancy of voltage drop is maintained over a very wide range of currents. For discharges produced by 4- $\mu$ sec voltage pulses, the transition from the high-voltage form to the arc takes place only at currents exceeding 1000 amp.

**I**N UNIFORM ELECTRIC FIELDS, the striking voltage for a discharge satisfies the similarity rule; i.e., it is a function of the product  $pd$ , where  $p$  is the pressure and  $d$  the distance between electrodes. A number of investigations<sup>1,2</sup> have shown noticeable deviations from the similarity rule when the electric field at the cathode begins to exceed

$10^6$  v/cm, and spontaneous emission of electrons begins. This situation may arise either at very high gas pressures, on the order of tens of atmospheres, where the electrode voltage reaches hundreds of kilovolts, or at very small gap widths where even at a few hundred volts the field strength at the cathode reaches the above-mentioned figure. In the work re-